Chapter 12: 'Frequency Noise and Linewidth of Mid-Infrared Continuous-Wave Quantum Cascade Lasers: An Overview' in 'The Wonders of Nanotechnology. Quantum and Optoelectronic Device...

Chapter · January 2015

CITATIONS
0

READS
258

4 authors, including:

Stéphane Schilt
Université de Neuchâtel
146 PUBLICATIONS **1,954** CITATIONS
SEE PROFILE

Lionel Tombez
IBM
24 PUBLICATIONS **210** CITATIONS
SEE PROFILE

Daniel Hofstetter
Université de Neuchâtel
262 PUBLICATIONS **5,691** CITATIONS
SEE PROFILE

Published in M. Razeghi, L. Esaki, and K. von Klitzing, Eds.,
The Wonders of Nanotechnology: Quantum and Optoelectronic Devices and Applications (chapter 12),
261-287, 2013
which should be used for any reference to this work

Chapter 12
Frequency Noise and Linewidth of Mid-infrared Continuous-Wave Quantum Cascade Lasers: An Overview

Stéphane Schilt, Lionel Tombez, Gianni Di Domenico, and Daniel Hofstetter
Laboratoire Temps-Fréquence, Université de Neuchâtel, Neuchâtel, Switzerland

12.1 Introduction

Since their first demonstration in 1994,[1] quantum cascade lasers (QCLs) have shown remarkable improvements in terms of technology and overall performance. The first devices were operated in pulsed mode only, at cryogenic temperatures, with a multimode emission and a tiny average output power. In less than one decade, advancements in the design, fabrication, and

processing of QCLs have led to important achievements, such as pulsed operation at room temperature,[2] strong reduction in the threshold current and dissipated electrical power, single-mode continuously tunable emission with distributed-feedback (DFB) gratings,[3] continuous-wave (CW) operation at cryogenic temperature in a first step and at room temperature currently in several spectral ranges,[4] as well as a high output power (up to several hundreds of milliwatts in single-mode operation). All of these milestones made QCLs very versatile laser sources in the mid-infrared spectral region, leading to applications in various fields covering, e.g., defense (directional infrared countermeasure systems for civil and military aircrafts) or free-space optical communications.[5] However, their broad spectral coverage over the important mid-infrared fingerprint region has so far resulted in the most widespread use of QCLs in the field of high-precision and high-resolution spectroscopy and trace gas sensing. Owing to their nice spectral properties as well as their fast tuning and direct-modulation capabilities via their injection current, QCLs have been implemented in many sensitive spectroscopy techniques, such as long path length,[6] balanced detection,[7] wavelength-modulation spectroscopy,[8] frequency-modulation spectroscopy,[9] photoacoustic or quartz-enhanced photoacoustic spectroscopy,[10,11] and cavity ring-down spectroscopy.[12]

An essential requirement for high-resolution spectroscopy applications and trace gas sensing is the spectral purity of the laser source, which needs to be single mode and narrow linewidth. For a QCL, this implies CW operation because pulsed operation leads to an important chirp of the QCL frequency that results from the thermal heating of the laser structure during the current pulses.[13] Even with extremely short pulses of 5 ns, an effective QCL linewidth in the range of 250 MHz has typically been observed,[14] whereas longer pulses (10–50 ns) can lead to a linewidth broader than 1 GHz,[15,16] which becomes similar to the typical width of rovibrational transitions of small molecules at atmospheric pressure.[17] Continuous wave DFB QCLs have a much narrower linewidth in the 1- to 10-MHz range.[18–24] This is most often fully adequate for trace gas sensing but may still be a limiting factor in some particular high-resolution spectroscopy applications. As a typical example, Bartalini et al. reported that the molecular linewidth of a Doppler-free CO_2 transition at 4.3 μm obtained by polarization spectroscopy was larger than expected, limited by the emission linewidth of the DFB QCL used in their setup.[25] In their comb-assisted spectroscopy experiments of CO_2 at 4.3 μm, performed with a QCL referenced to a mid-infrared optical frequency comb, Gambetta et al.[26] also mentioned that the precision of the determined CO_2 self-broadening coefficient was limited by the emission linewidth of their DFB QCL. Finally, in the very recent demonstration by Hugi et al.[27] of a mid-infrared frequency comb directly generated from a broadband QCL, the linewidth of an individual QCL comb mode could not be assessed from the heterodyne beat

with a reference CW QCL, since the beat linewidth was dominated by the contribution of the CW laser.

Therefore, many applications would greatly benefit from QCLs with narrower linewidth, and the development of such lasers is of significant interest for high-resolution spectroscopy. External cavity (EC) QCLs have been developed, achieving a large tuning range of over 15% of their central wavelength,[28] but so far without significant improvement in terms of linewidth as compared to DFB QCLs.[29] In order to develop QCLs with narrower linewidth, the mechanisms contributing to the linewidth need to be better understood. Generally speaking, fluctuations of the laser emission frequency occurring at different timescales are responsible for the broadening of the linewidth. These fluctuations are characterized by the laser frequency noise power spectral density (PSD), expressed in units of Hz^2/Hz. Until recently, this quantity has been studied and optimized very little in QCLs. This is in sharp contrast to the other parameters that are more commonly considered, such as the output power or the wavelength tuning, to name a few. However, there has been a growing interest during the last couple of years for this topic, ranging from basic studies of the frequency noise in QCLs at either cryogenic[19] or room temperature,[20,21,24] to studies of its dependence as a function of the laser temperature,[22] and investigations of its possible origin,[22,23] as well as studies in relation to the frequency stabilization of mid-infrared QCLs.[30–33]

In this chapter, we present an overview of experimental results obtained in recent years on the frequency noise of QCLs. The overview is based on a compilation of both our own work and studies from other laboratories. We also briefly discuss the frequency noise reduction obtained by different active stabilization methods. First of all, we begin in Section 12.2 with a short reminder about the relation between frequency noise and linewidth in a laser and show how the frequency noise spectrum of a QCL can be experimentally measured. Then we discuss the intrinsic linewidth of QCLs in Section 12.3 and the impact of technical noise on the experimentally observed linewidth in Section 12.4. Subsequently, we revisit the experimental results on the frequency noise measured in different QCLs reported worldwide (Section 12.5), and we present our study of the temperature dependence of the frequency noise in a 4.6-μm QCL (Section 12.6). Finally, Section 12.7 mentions some aspects of the origin of frequency noise in QCLs.

12.2 Frequency Noise and Laser Linewidth in QCLs: Experimental Methods

12.2.1 Relation between frequency noise and laser linewidth

It is convenient to characterize the spectral purity of a laser by the full width at half maximum (FWHM) linewidth of the optical lineshape. The linewidth can

be directly measured from the heterodyne beat between the laser under test and a reference laser or from self-homodyning using a long-delay-line interferometer.[34] This method is straightforwardly applicable to near-infrared lasers but not to QCLs due to the lack of low-loss and affordable optical fibers in the mid-infrared spectral region.

The linewidth is a single value that is adequate for a rough comparison of the spectral properties of different lasers, but it gives a very incomplete view of the spectral distribution of the laser frequency noise. On the other hand, complete information is given by the laser frequency noise PSD $S_{\delta\nu}(f)$, which represents the spectral distribution of the laser frequency fluctuations. Knowing the frequency noise PSD of a laser, its exact lineshape and the corresponding linewidth can be calculated with the two-step integration introduced by Elliott et al.[35] and discussed later on by other authors:[36–38]

$$S_E(\nu) = 2\int_{-\infty}^{\infty} e^{-i2\pi\nu\tau}\left[E_0^2 e^{i2\pi\nu_0\tau}\exp\left(-2\int_0^{\infty} S_{\delta\nu}(f)\frac{\sin^2(\pi f\tau)}{f^2}df\right)\right]d\tau. \quad (12.1)$$

The first integration step consists of calculating the autocorrelation function $\Gamma_E(\tau)$ of the electrical field, which is represented by the term in the square brackets in Eq. (12.1). Then, the optical spectrum $S_E(\nu)$ is obtained in the second step by a Fourier transform of $\Gamma_E(\tau)$. Equation (12.1) can be analytically solved only in the simple case of a pure-white frequency noise $S_{\delta\nu}(f) = S_0$,[36] leading to the well-known Lorentzian lineshape with a FWHM $\Delta\nu_L = \pi S_0$. In all other cases, including any real laser frequency noise spectra encountered in practice, Eq. (12.1) must be numerically integrated. As discussed in Ref. 39, this procedure is not straightforward, and great care is needed in its implementation to obtain the correct laser optical lineshape without any numerical artifact. In order to circumvent this numerical integration, we introduced a simple approximation to determine the linewidth of a laser from an arbitrary frequency noise spectrum, based on the concept of the β-separation line that divides the frequency noise PSD into two geometrical surfaces with a strongly different impact on the laser lineshape.[40]

The β-separation line is defined as $S_{\delta\nu}(f) = (8\ln(2)/\pi^2)\cdot f$. It is a line of slope $\sim$0.56 in the linearly plotted frequency noise PSD. Only the noise components for which $S_{\delta\nu}(f) > (8\ln(2)/\pi^2)\cdot f$ (corresponding to the slow-modulation area) contribute to the linewidth of the signal, whereas the components for which $S_{\delta\nu}(f) < (8\ln(2)/\pi^2)\cdot f$ (fast-modulation area) only affect the wings of the lineshape, without contributing to the linewidth. The FWHM linewidth can thus be approximated from the surface A of the slow-modulation area (see Fig. 12.1):

$$FWHM = \sqrt{8\ln(2)A}. \quad (12.2)$$

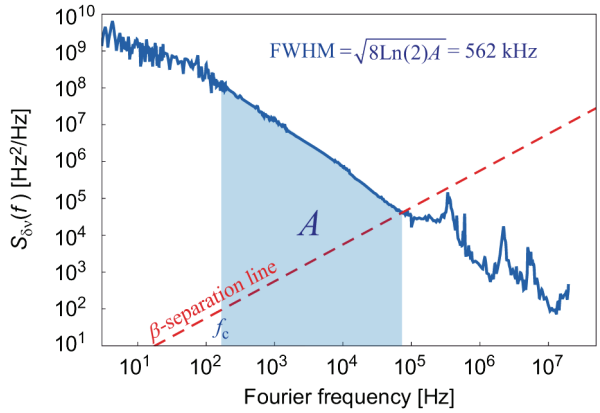

Figure 12.1 Measured frequency noise spectrum of a 4.6-μm DFB QCL composed of flicker (1/*f*) noise. An approximate linewidth is obtained from the surface *A* (colored area in the plot) of the slow-modulation area for which the frequency noise PSD exceeds the *β*-separation line (dashed red line). A low-frequency cutoff $f_c = 200$ Hz ($\tau_o = 5$ ms) is introduced in the calculation of the surface *A* to prevent the divergence of the surface and of the retrieved linewidth for infinite observation times (adapted from Ref. 24).

The surface A is the geometrical area under the frequency noise PSD obtained for all Fourier frequencies for which $S_{\delta\nu}(f)$ exceeds the β-separation line.[40] In the case of a typical frequency noise spectrum dominated by flicker ($1/f$) noise, as displayed in Fig. 12.1 for a DFB QCL at 4.6 μm, a cutoff frequency f_c (inverse of the observation time τ_o in which the linewidth is measured, $f_c = 1/\tau_o$) needs to be introduced to prevent the divergence of the surface A at low frequency. An experimental validation of the approximated linewidth given by Eq. (12.2) proved its accuracy (within the experimental uncertainties) over more than three decades of linewidth values.[39] In the example of Fig. 12.1, the linewidth of the DFB QCL approximated using Eq. (12.2) is around 900 kHz for a cutoff frequency of 1 Hz (1-s observation time) and 560 kHz for a cutoff frequency of 200 Hz (5-ms observation time).

12.2.2 Frequency noise measurement methods

Different methods can be used to measure the frequency noise spectrum of a laser. One technique makes use of an optical frequency discriminator to convert the laser frequency fluctuations into intensity fluctuations. An optical frequency discriminator is a device having a frequency-dependent transmission or reflection in a restricted frequency range. A molecular transition in a gas-filled absorption cell has been the most common optical frequency discriminator used with QCLs in the mid-infrared. Alternatively, a resonance of an optical Fabry–Pérot cavity can be used in a similar

manner, but this has been rarely implemented with QCLs in the mid-infrared, in contrast to the near-infrared where the method is quite common owing to the much easier availability of Fabry–Pérot cavities. N_2O at 8.5 μm,[41] CO_2 at 4.3 μm,[19,21,23] or CO at 4.6 μm[20,22,24] are some examples of reported molecular frequency discriminators. This method has also been implemented recently with a terahertz QCL using a Doppler-broadened methanol molecular transition.[42] The laser under test is generally tuned to the side of the absorption line, to a linear region where frequency fluctuations are linearly converted into intensity fluctuations that are subsequently measured with a photodiode. Reduced cell pressure operation is required to achieve a narrow-linewidth absorption feature, providing a high conversion factor of frequency noise into intensity noise (the so-called discriminator slope). The discriminator slope must be sufficiently high that the contribution of the frequency noise converted into intensity noise is much larger than the direct contribution of the laser intensity noise, which also impacts the detector signal. The parameters of the gas cell (path length, gas pressure) must therefore be properly selected in order to optimize the discriminator slope.[24]

The experimental setup implemented in our studies is shown in Fig. 12.2. The strongly divergent QCL emission is collimated with an aspheric ZnSe

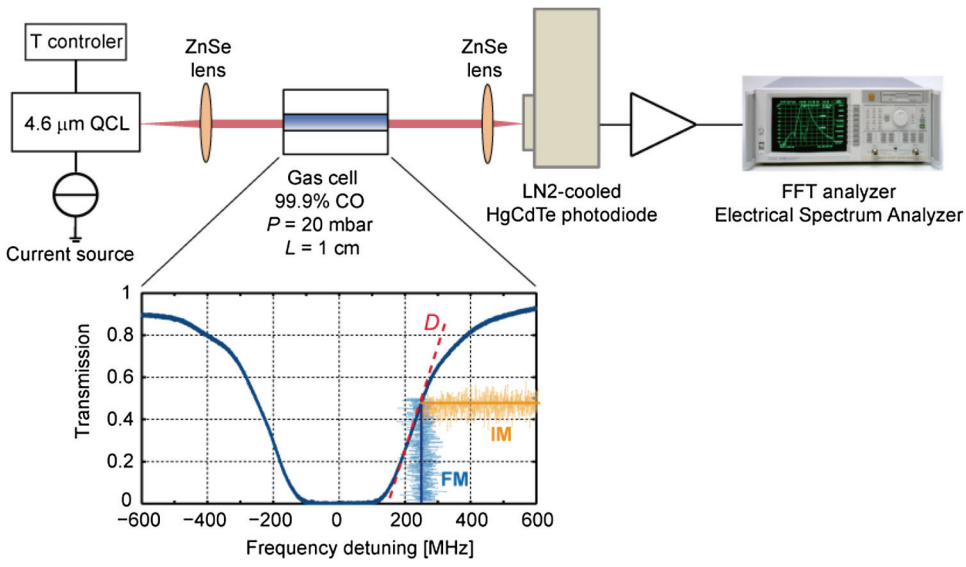

Figure 12.2 Scheme of the experimental setup used to measure the frequency noise of a QCL at 4.6 μm. The R(14) CO absorption profile measured in the gas cell is shown in the lower part of the figure. The linear side of the absorption profile is used as a frequency discriminator to convert frequency noise (FM) into intensity noise (IM). The discriminator slope *D* is indicated by the dashed line.

lens, then passes through the gas-filled absorption cell and is finally focused onto a low-noise HgCdTe photodiode. The cell is only 1-cm long and is filled with pure CO at a pressure of about 20 mbar, which is sufficient to produce a high absorption, as a result of the intense linestrength of the CO lines in the fundamental vibrational band. The voltage fluctuations of the photodiode output signal are measured with a fast Fourier transform (FFT) spectrum analyzer for Fourier frequencies of up to 100 kHz and with an electrical spectrum analyzer (ESA) at higher frequencies. The PSD of the photodiode output voltage is converted into frequency noise PSD of the laser by scaling with the squared value of the measured discriminator slope D, which is determined from the recorded cell transmission spectrum obtained when scanning the laser through the absorption line. A linear fit of the side of the molecular transmission profile provides the discriminator slope, as shown in Fig. 12.2 for the R(14) rovibrational transition of CO at 2196.6 cm^{-1}.

A second method to measure the frequency noise spectrum of a laser is by beating the laser under test with a reference laser and by analyzing the frequency noise of the radio-frequency (RF) beat with an RF discriminator. The method is particularly attractive at wavelengths where a proper optical discriminator is not available, but the price to pay is the need for a second laser. This reference laser is either similar to the first one or has a much smaller frequency noise. In the first case, the two lasers are considered to contribute equally to the noise of the RF beat, and the frequency noise PSD of the beat signal is twice that of a single laser. In the second case, the frequency noise PSD of the laser under test is directly obtained since the noise of the reference laser is negligible. An RF discriminator has been successfully implemented to characterize near-infrared lasers[43,44] but, to the best of our knowledge, has not been used so far with QCLs.

Finally, a third method to measure the frequency noise spectrum of a QCL was recently proposed by Knabe et al.,[29] based on the characterization of the instantaneous optical frequency of an EC QCL by comparison to a near-infrared optical frequency comb. The near-infrared fiber comb centered at 1550 nm was combined with the 4.5-μm QCL in a nonlinear crystal to generate a new frequency comb at 1150 nm by sum-frequency generation. This new comb combines the frequency properties of the QCL and of the near-infrared comb. The frequency fluctuations of the QCL were obtained by a subsequent heterodyning of the 1150-nm comb with a supercontinuum comb generated from the spectrally broadened near-infrared comb. The resulting beat signal contains mainly the frequency fluctuations of the QCL, the contribution of the comb repetition rate being negligible for a stabilized comb. The beat signal was digitized and processed to extract the QCL instantaneous frequency and its frequency noise spectrum.

12.3 Intrinsic Linewidth in QCLs

The intrinsic (or "instantaneous") linewidth of a laser is due to spontaneous emission in the gain medium. Spontaneous emission gives rise to a white frequency noise PSD, which leads to a Lorentzian lineshape with a theoretical linewidth given by the Schawlow–Townes formula,[45] modified by C. H. Henry to account for the coupling between amplitude and phase noise in semiconductor lasers:[46]

$$\Delta\nu_{ST} = \frac{v_g^2 h\nu n_{sp}\alpha_{tot}\alpha_m(1+\alpha_e^2)}{4\pi P_0}. \tag{12.3}$$

Here, v_g is the group velocity, n_{sp} the spontaneous emission factor, α_{tot} the total losses in the cavity, α_m the mirror losses, α_e the linewidth enhancement factor,[46] and P_0 the output power. QCLs are known to have a narrow intrinsic linewidth that results from their tiny linewidth enhancement factor α_e and from the presence of ultrafast radiative processes.[47] The linewidth enhancement factor accounts for the variations in the refractive index of the gain medium due to fluctuations of the carrier density. It has quite a large value of typically 2 to 10 in interband diode lasers,[48] resulting from the asymmetry of the gain curve, which leads to a broadening by a factor $(1 + \alpha_e^2)$ of the intrinsic linewidth compared to the Schawlow–Townes formula. In contrast, the gain curve is symmetric in QCLs because of the intersubband transition between discrete levels, both located in the conduction band. As a consequence, the linewidth enhancement factor is expected to be close to zero, which was indeed experimentally observed.[49] Even if this is strictly valid in a DFB QCL only when the laser emission line is centered exactly to the gain peak (i.e., when the DFB grating is tuned to the gain peak), the α_e factor remains small when the DFB grating is only slightly detuned from the gain curve. This implies that the major current-tuning mechanism in a QCL is of thermal origin (dependence of the gain curve and DFB grating with respect to the dissipative heating induced by the driving current). A second important consequence of the small α_e factor in QCLs in the context of this paper is that current noise induces frequency noise via thermal mechanisms.

Because of the presence of $1/f$ noise at low frequency, the white frequency noise of a QCL can be observed only as a high-frequency plateau. Bartalini et al. experimentally observed an upper limit of 163 Hz^2/Hz for the white frequency noise of a 4.33-μm DFB QCL operated at cryogenic temperature (85 K) at Fourier frequencies around 100 MHz, corresponding to an intrinsic linewidth of about 510 Hz.[19] The frequency noise spectrum of the room-temperature DFB QCL displayed in Fig. 12.1 shows an upper limit for the white frequency noise of roughly 100 Hz^2/Hz (at 10 MHz), even though one cannot certify that the white frequency noise level is reached in this measurement due to the limited detector bandwidth. This corresponds to an

upper limit for the intrinsic linewidth of ~300 Hz, a value that is interesting to compare with the theoretical linewidth given by Eq. (12.3). As already mentioned, the linewidth enhancement factor α_e is close to zero in a QCL, and one can reasonably consider $\alpha_e = 0$ in Eq. (12.3). A delicate aspect in properly evaluating the Schawlow–Townes linewidth for a DFB QCL lies in the difficulty in determining both the total cavity losses $\alpha_{tot} = \alpha_m + \alpha_{wg}$ (mirror and waveguide) and the mirror losses α_m to compute the intracavity optical power from the output power P_0. It is not correct to consider the losses of a Fabry–Pérot laser, which can be straightforwardly determined. This may lead to an overestimation of the theoretical linewidth because the losses of the grating (α_{DFB}) need to be accounted for in a DFB laser, and these losses are generally lower than the mirror losses in a Fabry–Pérot laser. The total losses in our DFB QCL were estimated by comparing its threshold current with those of a similar Fabry–Pérot device (same manufacturer and close design, but with slightly different dimensions), assuming that the ratio of the total losses coincides with the ratio of the threshold currents. Considering similar waveguide losses $\alpha_{wg} \approx 4.5\ \text{cm}^{-1}$ in both cases (as measured by the manufacturer on Fabry–Pérot devices), the grating losses are estimated to $\alpha_{DFB} = 1.47\ \text{cm}^{-1}$, which is in relatively good agreement with data reported for a 9-μm DFB QCL ($\alpha_{wg} = 6.7\ \text{cm}^{-1}$, $\alpha_{DFB} = 0.7\ \text{cm}^{-1}$).[50] For comparison, the mirror losses in the Fabry–Pérot laser were higher: $\alpha_m = 2.7\ \text{cm}^{-1}$. With a spontaneous emission coefficient $n_{sp} = 1$, an optical power $P_0 = 6$ mW, and using typical values of the laser parameters provided by the manufacturer, an intrinsic linewidth $\Delta\nu_{ST} \approx 380$ Hz is obtained. This value is very slightly affected by the only partial knowledge of the waveguide losses in the Fabry–Pérot laser, as changing these losses in the range of 4 to 5 cm^{-1} only changes the computed intrinsic linewidth by a couple of hertz. The calculated theoretical linewidth is thus in good agreement with the value of ~300 Hz assessed from the frequency noise spectrum.

12.4 Impact of Technical Noise on the QCL Experimental Linewidth

Despite the extremely narrow intrinsic linewidth of QCLs discussed in Section 12.3, the real linewidth observed in practical applications is much broader, in the megahertz or submegahertz range in the best case,[24] which means that the intrinsic linewidth is never observed in practice. This is a consequence of the flicker noise that affects any free-running QCL at low Fourier frequency, as well as most other semiconductor devices. Here, we discuss a prerequisite to achieving a narrow linewidth in a QCL: the need to not be limited by technical noise external to the QCL. This includes both laser temperature and driving current. Any temperature or current variation translates into a fluctuation of the laser frequency via the temperature- and current-tuning coefficients of the

laser, $\Delta\nu/\Delta T$ and $\Delta\nu/\Delta I$, respectively. These are typically on the order of 5 GHz/K and 0.3–1 GHz/mA in DFB QCLs at 4- to 5-μm wavelength. An average temperature stability of the laser of ±0.01 K is usually sufficient and is achievable with a standard regulation loop that includes a thermoelectrical cooler and a negative thermal coefficient resistor as a temperature sensor. Temperature variations arise on a long timescale and only induce a slow drift of the laser emission frequency.

Much more attention must be paid to the current source that drives the laser because the current noise of the driver can degrade the laser frequency noise and therefore broadens the linewidth to a significant extent. A low-noise driver is required to observe the frequency noise originating from the QCL itself. We refer to this frequency noise as the noise *inherent* to the laser (not to be confused with the intrinsic noise that is responsible for the intrinsic linewidth discussed in Section 12.3), without limitation from the current noise of the driver. In Ref. 24, we experimentally compared the impact of two different current sources on the frequency noise and linewidth of a 4.6-μm DFB QCL. The current noise of these two drivers was measured on a resistive load (30 Ω) at the same voltage and current used to drive the QCL. The current noise spectral density is shown in Fig. 12.3(a). The first driver (labelled Driver-1) has a white current noise of about 2 nA/Hz$^{1/2}$, whereas the second driver has an average noise floor of ∼350 pA/Hz$^{1/2}$ (and even ∼200 pA/Hz$^{1/2}$ in the range of 1–10 kHz). The impact on the laser frequency noise is clearly visible in Fig. 12.3(b): Driver-1 induces an excess frequency noise in the range of 1 kHz to 3 MHz. The contribution of the current source to the laser frequency noise, calculated from the white current noise and combined with the dynamic frequency response of the laser, is also displayed in Fig. 12.3(b). This current noise fully explains the observed excess frequency noise, which leads to a laser linewidth of about 1.5 MHz (at 5-ms observation time).

On the other hand, the laser frequency noise spectrum obtained with Driver-2 corresponds to the noise inherent to the laser, without any degradation induced by the driver, apart from the small bumps visible around 400 kHz and at higher frequencies. The corresponding linewidth is ∼550 kHz (5-ms observation time), a factor of ∼3 narrower than with the use of Driver-1. The importance of having a low-noise current source to reach the frequency noise inherent to the QCL and avoid any excess noise clearly appears in these results. They show that a current noise of roughly 2 nA/Hz$^{1/2}$ already broadens the laser linewidth by a factor ∼3.

The maximum tolerable driver-current noise that enables the inherent noise of the laser to be reached without degradation from technical noise was simulated in Ref. 24 for a 4.6-μm DFB QCL. For this purpose, the impact of different levels of white-current noise on the QCL linewidth was calculated based on the formalism of Section 12.2.1. White current noise was considered because it is the most representative type of noise in typical laser drivers.

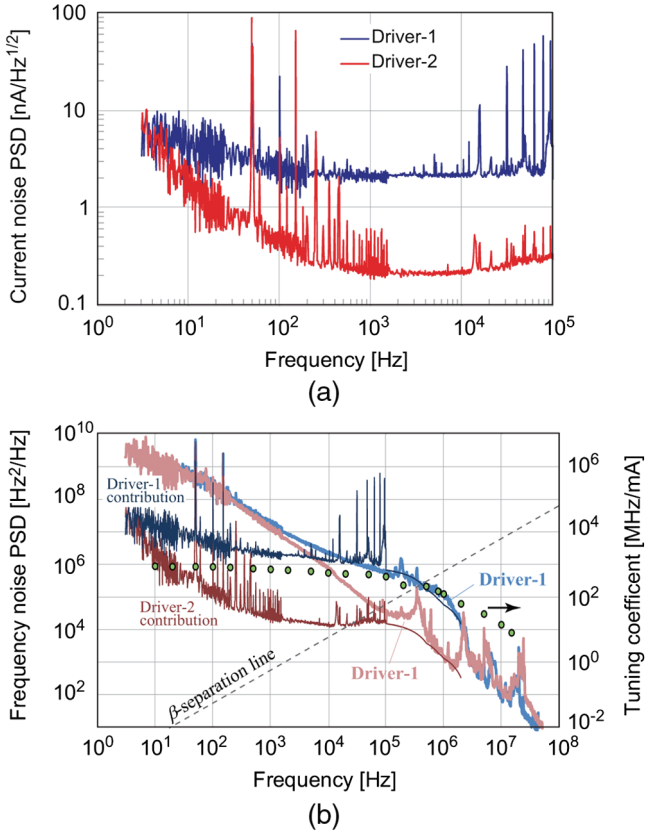

Figure 12.3 (a) Current noise spectral density of two QCL drivers. The noise peaks in the range of 10–100 kHz are experimental artifacts due to the measurement setup. The noise of Driver-2 below 100 Hz is limited by the 1/*f* instrumental noise floor. (b) Frequency noise of a 4.6-μm DFB QCL obtained with the use of two current drivers. The contribution of the drivers to the frequency noise is displayed as thin lines obtained by combining the current noise with the measured laser transfer function (shown by green circles on the right vertical scale). (See color plate section.)

The contribution of the current noise to the laser frequency noise was calculated taking into account the dynamic frequency response of the laser. Figure 12.4(a) shows the calculated frequency noise corresponding to three different levels of current noise: 350 pA/Hz$^{1/2}$, 2 nA/Hz$^{1/2}$, and 10 nA/Hz$^{1/2}$. The first two values correspond to the noise of the two aforementioned laser drivers, whereas the highest current noise of 10 nA/Hz$^{1/2}$ typically corresponds to some commercial QCL drivers. The calculated impact of the driver current noise on the QCL linewidth is shown in Fig. 12.4(b). One notices that the linewidth is unaffected for current noise densities <0.5 nA/Hz$^{1/2}$ but drastically increases at a rate of $\sim$1.6 MHz/(nA/Hz$^{1/2}$) for current noise >1 nA/Hz$^{1/2}$.

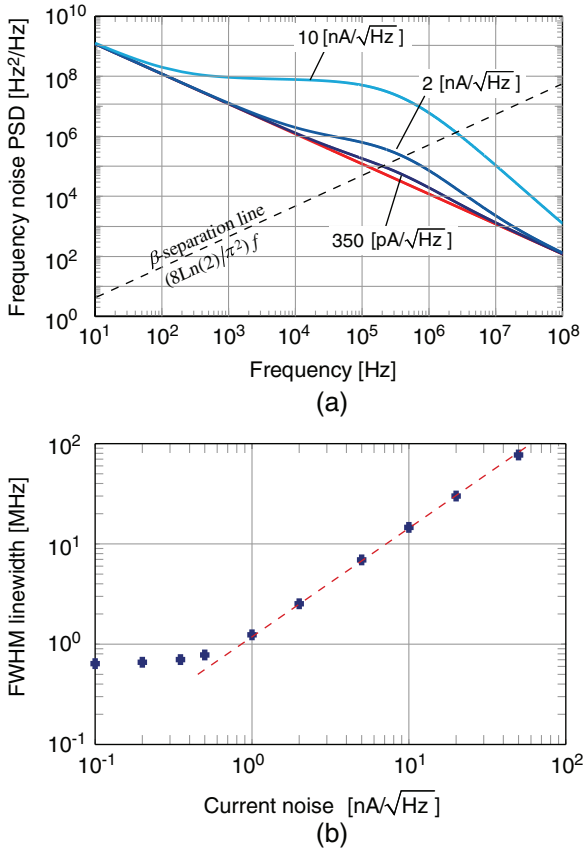

Figure 12.4 (a) Simulation of the laser frequency noise induced by drivers with different current noise densities. (b) Calculated laser linewidth (FWHM) as a function of the driver current noise density (white current noise is considered). The dashed line represents the linear broadening rate [~1.6 MHz/(nA/Hz$^{1/2}$)] of the laser linewidth as a function of the current noise (reprinted from Ref. 24).

12.5 Overview of Reported Frequency Noise Spectra in 4- to 5-μm QCLs

In this section, we first review and discuss the main results obtained so far on the frequency noise of free-running QCLs in the 4- to 5-μm spectral range (Section 12.5.1). In Section 12.5.2, we discuss some accomplishments in frequency stabilization of QCLs, for which the initial frequency noise of the unlocked laser plays an important role in the achievable performances of the stabilized laser.

12.5.1 Free-running QCLs

Since 2010, at least four different studies have been published about the frequency noise of DFB QCLs in the 4- to 5-μm range, between our group in

Table 12.1 Comparison of different studies performed during recent years on the frequency noise of 4- to 5-μm QCLs (DFB or EC). The reported linewidth is usually determined from the frequency noise spectrum using either the exact numerical integration of Eq. (12.1) or the approximation given by Eq. (12.2) for an observation time in the range of 1 to 10 ms. [RT: room temperature (unspecified value).]

Laser type	λ (μm)	T_{op} (K)	Manufacturer	Discriminator	FWHM (MHz)	Group	Ref.
DFB	4.33	85	Alpes Lasers	CO_2 line	~6	LENS (I)	19
DFB	4.55	277	Alpes Lasers	CO line	0.6	Our work	20
DFB	4.36	288	Hamamatsu	CO_2 line	0.4	LENS (I)	21
DFB	4.48–4.55	128–303	Alpes Lasers	CO line	10–0.8	Our work	22
EC	4.5	RT	Daylight Solutions	Beat with comb	4	NIST (USA)	29

Neuchâtel, Switzerland and LENS in Florence, Italy. In addition, the frequency noise of an EC QCL was recently reported by a research group at National Institute of Standards and Technology (NIST), USA. Table 12.1 summarizes the main characteristics of each of these studies.

The first paper from the LENS group reported the frequency noise and intrinsic linewidth of a DFB QCL from Alpes Lasers, operated at cryogenic temperature (85 K) and emitting at 4.33 μm.[19] A gas cell filled with CO_2 was used as a frequency discriminator. Then, we reported the first measurement of the frequency noise spectrum of two 4.55-μm DFB QCLs operated at room temperature.[20] The DFB QCLs were both produced from the same fabrication run and supplied by Alpes Lasers. In this case, a Doppler-broadened transition of CO was used as a frequency discriminator. The two lasers showed a very similar frequency noise spectrum, as shown in Fig. 12.5, even though they were operated at slightly different temperatures and currents to reach the CO line. Surprisingly, the frequency noise in these two lasers was two orders of magnitude lower than that of the cryogenic QCL of LENS, leading to a one-order-of-magnitude-narrower linewidth. The linewidth calculated from the frequency noise spectrum using the formalism described in Section 12.2.1 was around 600 kHz for each laser (at 10-ms observation time), which is one of the narrowest linewidths achieved for a free-running QCL over a millisecond timescale. The heterodyne beat of a width of ~1 MHz (FWHM) measured between the two lasers shown in the inset of Fig. 12.5 is in good agreement with the linewidth assessed from the frequency noise spectra.

Our observation of a sub-megahertz linewidth for the room-temperature 4.55-μm DFB QCL was followed by a similar result obtained in LENS for another DFB QCL at 4.3 μm, also operated at room temperature, but produced by a different supplier (Hamamatsu).[21] In comparison, the first cryogenic QCL characterized in LENS had a linewidth of about 6 MHz.

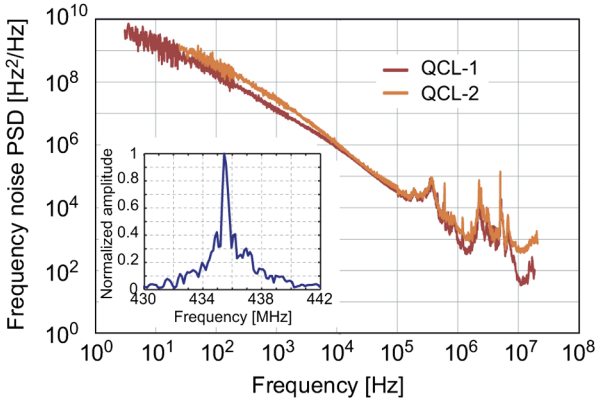

Figure 12.5 Frequency noise spectra of two similar DFB QCLs from the same fabrication run, operated in slightly different conditions (QCL-1: $T = 5$ °C, $I_{op} = 350$ mA; QCL-2: $T = -5$ °C, $I_{op} = 400$ mA). The excess noise at high frequency (around 400 kHz and above 1 MHz) is due to technical noise induced by the laser driver. Inset: heterodyne beat-note signal between the two QCLs, showing a beat linewidth of <1 MHz. (See color plate section.)

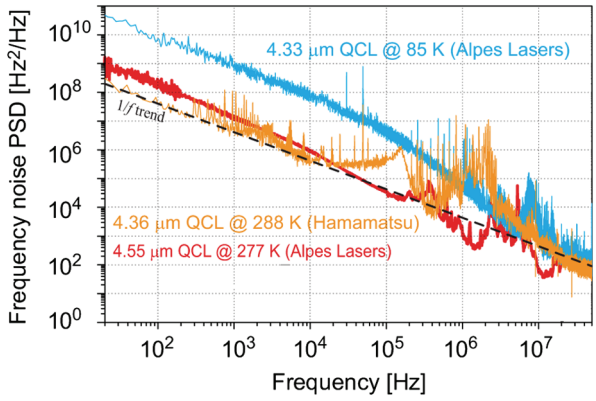

Figure 12.6 Comparison of the frequency noise PSD reported for different DFB QCLs in the 4.3- to 4.6-μm range, operated at cryogenic temperature [blue curve (from Ref. 19)] and room temperature [red and orange curves (from Refs. 20 and 21, respectively, courtesy of S. Bartalini, LENS)]. (See color plate section.)

Figure 12.6 shows a comparison of the frequency noise spectra obtained for the three aforementioned DFB QCLs in the Fourier frequency range from 20 Hz to 50 MHz. The two lasers operated at room temperature show a rather similar $1/f$ noise spectrum, whereas the cryogenic QCL has a two-orders-of-magnitude-higher noise at low frequency, namely up to 100 kHz. At higher frequencies, the noise dependence turns into a $1/f^2$ regime in the cryogenic QCL, and the three lasers seem to reach a similar white frequency noise floor at high frequency. These results may indicate a general influence of

temperature on the frequency noise of QCLs, but it is difficult to draw definitive conclusions from these results, mainly because they were obtained with different devices and thus were probably influenced by other parameters such as their different dimensions, design, and fabrication process. Therefore, the temperature dependence of the frequency noise of a single QCL was investigated in a broad temperature range and is described in Section 12.6.

12.5.2 Frequency-stabilized QCLs

In order to achieve narrower linewidths as required for high-resolution spectroscopy applications, active frequency stabilization techniques can be implemented. The achievable linewidth reduction depends on the stabilization bandwidth, the noise of the frequency reference used to stabilize the QCL, and also on the frequency noise PSD of the free-running QCL. Frequency stabilization of QCLs has been accomplished by various means over the last decade.

The first realization was reported by R. M. Williams et al.[51] Using a molecular side-locking approach with an electronic feedback to the QCL current controller, they stabilized an 8.5-μm DFB QCL to a rovibrational transition of N_2O and achieved a linewidth of 12 kHz calculated from the frequency noise of an out-of-loop error signal.

M. S. Taubman et al.[52] stabilized two QCLs at 8.5 μm to optical cavities using the Pound–Drever–Hall method. By further locking one cavity to the other one, they achieved a linewidth of 5.6 Hz in the beat between the two lasers. However, this represents a relative linewidth since the two lasers were not independent but locked together via the cavities. The noise of the optical cavities was therefore common to the two lasers and canceled out in the beat signal. The absolute linewidth of each stabilized QCL was most likely much broader. A cavity-stabilized QCL was used in noise-immune cavity-enhanced optical-heterodyne molecular spectroscopy (NICE-OHMS) experiments.[53] Phase locking of a 9.2-μm DFB QCL to a single-mode CO_2 laser was realized by F. Bielsa et al.[54] With this scheme, they were able to reduce the QCL linewidth to the level of the CO_2 laser, i.e., to the kilohertz range.

The most recent advances in the field of QCL frequency stabilization consists of linking a QCL to an optical frequency comb in order to transfer the absolute frequency accuracy of the comb to the QCL and to simultaneously reduce its linewidth, e.g., for extremely accurate determination of line-center frequencies and line profile parameters of molecular transitions. Sum- or difference-frequency generation processes have been used to link a QCL to a near-infrared fiber-laser comb,[30] to a visible Ti:sapphire comb,[31] or to a thulium comb.[32] In the first two cases, the comb was referenced to an atomic clock. The stabilization of the QCL to the comb was conventionally achieved by phase locking the beat note (between the laser and the comb) to a reference oscillator[30] in order to ensure long-term stability and accuracy, but without

reducing the QCL linewidth. In contrast, optical injection locking has been recently demonstrated for the first time to link a 4.67-μm QCL to a frequency comb.[31] In this case, a significant reduction of the QCL linewidth to 40 kHz was achieved. A linewidth of 25 kHz (at 1-ms observation time) was also achieved by phase locking a 9-μm QCL to a thulium comb.[32] However the comb was free-running in this case, so an absolute frequency accuracy of the QCL was not achieved.

Finally, a subkilohertz linewidth was reported for a 4.3-μm DFB QCL stabilized to a sub-Doppler CO_2 transition by polarization spectroscopy.[33] The linewidth and frequency accuracy of the stabilized QCL was assessed from the beat signal with a frequency comb.

12.6 Temperature Dependence of the Frequency Noise in a QCL

The temperature dependence of the flicker frequency noise in a DFB QCL has been recently investigated.[22] In this work, we studied for the first time the frequency noise of the same device operated over a wide range of temperatures, extending from 128 to 303 K. The DFB QCL, emitting in the range of 4.48 to 4.55 μm, was provided by Alpes Lasers. It uses a buried heterostructure active region with epi-side-up mounting and benefits from a low-threshold current I_{th} ranging from 75 to 120 mA over the considered temperature range. The laser was placed in a cryostat and was driven by a low-noise current source (with ~350-pA/Hz$^{1/2}$ current-noise PSD) that did not contribute to the laser frequency noise, as discussed in Section 12.4. The minimum operating temperature of the laser was restricted to 128 K because of the increasing voltage across the QCL at low temperature that eventually reached the 15-V compliance voltage of the driver.

Different rovibrational transitions of CO ranging from R(15) to R(24) were successively used as frequency discriminators to measure the frequency noise at the different laser temperatures. The laser drive current was adjusted to 50% above threshold in each case, and the discriminator slope was accurately measured at each temperature. Since previous studies made with QCLs at fixed temperatures showed a large difference in the frequency noise at low Fourier frequency, but not in the high-frequency white noise floor (see Fig. 12.6), the study of the frequency-noise temperature dependence was limited to Fourier frequencies below 100 kHz.

Figure 12.7 shows the frequency noise PSD of the QCL. The frequency noise PSD remains almost unchanged when the laser temperature is reduced from room temperature to ~200 K. However, it strongly increases at lower temperature and is enlarged by almost two orders of magnitude at 128 K. Additional measurements also showed that the frequency noise did not depend on the drive current I_0 in the QCL under test in the investigated

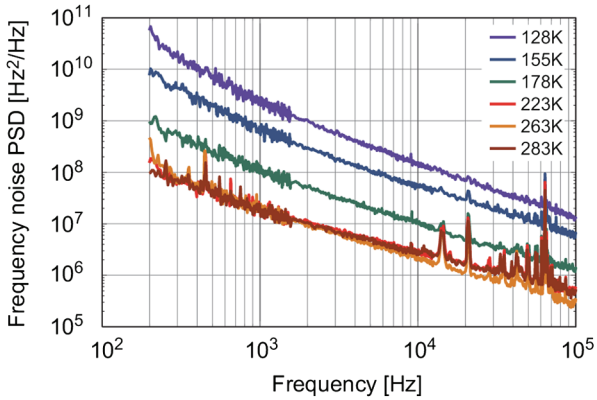

Figure 12.7 Frequency noise PSD of a 4.5-μm DFB QCL measured at different temperatures ranging from 128 to 283 K. The laser operating current was adjusted to $I_0/I_{th} \approx 1.5$ at each temperature (reprinted from Ref. 22). (See color plate section.)

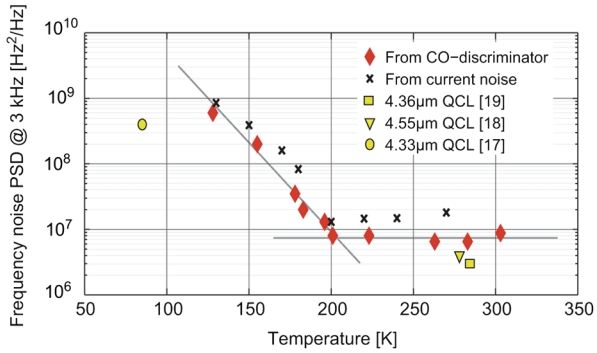

Figure 12.8 Temperature dependence of the frequency noise PSD in a DFB QCL measured at 3-kHz Fourier frequency (red diamonds). The gray lines result from a fit of the experimental data on both sides of the transition occurring at $T \approx 200$ K, corresponding to $S_{3\text{kHz}} = 7 \times 10^6$ Hz^2/Hz for $T > 200$ K and $S_{3\text{kHz}}(T) \approx 2 \times 10^{12}$ exp $(-0.06\ T)$ for $T < 200$ K. The black crosses represent the noise measured on the voltage across the laser, converted into an equivalent frequency noise using the laser differential resistance and the current-tuning coefficient (see discussion in Section 12.7). The yellow markers represent published values of QCL frequency noise obtained at different temperatures[19–21] (reprinted from Ref. 22). (See color plate section.)

current range $I_0/I_{th} = 1.2$–1.8. The frequency noise PSD at a particular Fourier frequency of 3 kHz, $S_{3\text{kHz}}$, was chosen as a parameter to characterize the temperature dependence of the laser frequency noise. Figure 12.8 shows the only temperature dependence of the frequency noise in a single QCL reported to date. The plot shows the existence of two very different regimes separated by an abrupt transition at ~200 K; above this point, the frequency noise PSD is almost independent of temperature, but it drastically increases

when the temperature is lowered below 200 K, with an exponential dependence with respect to temperature. Figure 12.8 also displays for comparison the former results obtained for different QCLs operated at a fixed temperature and discussed in Section 12.5.1 (see Fig. 12.6). The values obtained both at room temperature and at cryogenic temperature are in quite good agreement between the different lasers, despite their different characteristics (different design and fabrication parameters, different manufacturers, different operating parameters, etc.). This tends to indicate that the temperature dependence of the frequency noise in QCLs is related to some fundamental effect in the QCL semiconductor structure. But since only one laser has been ever studied over a wide range of temperatures, it is premature to draw such conclusions.

In terms of linewidth, the increase in laser frequency noise at low temperature translates into a large spectral broadening.[22] The linewidth broadens from ~770 kHz at room temperature to ~10 MHz at 128 K (at 5-ms observation time).

12.7 The Origin of Frequency Noise in QCLs

The content of Section 12.4 showed that the use of a low-noise current source enables the frequency noise inherent to the QCL to be achieved, without substantial degradation due to the laser driver. We discuss here some possible origins of this frequency noise, which thus result from one or several effects that are internal to the laser structure. S. Borri et al. first assumed the origin of flicker noise in QCLs to be internal to the laser.[23] They stated that "the $1/f$ noise in QCLs should arise from current fluctuations originating in the active medium by means of internal processes related to the peculiar QCL heterostructure." In order to support this assumption, they compared the frequency noise spectrum and the frequency tuning response in a cryogenic QCL and qualitatively observed a good overlap between these two quantities, which shows the same thermal cutoff at ~200 kHz. Stating that the same physical mechanism should govern these two quantities, they assumed an internal current noise to be responsible for this, although, without demonstrating it.

An experimental confirmation of this assumption has been shown in our investigations of the temperature dependence of the frequency noise in a QCL, described in detail in Ref. 22 and summarized in Section 12.6. In addition to the frequency noise optically measured at different temperatures using CO lines as frequency discriminators, we also measured the electrical noise in the laser, i.e., the voltage across the QCL, at the same temperatures. The measured voltage noise PSD was then converted into a current noise that we refer to as the laser *internal electrical noise*, using the corresponding laser differential resistance, also measured in our laser at various temperatures.

This internal electrical noise showed the same 1/*f* nature as the observed laser frequency noise. More importantly, it showed the same abrupt increase at temperatures below 200 K.

We evaluated the impact of this internal electrical noise by determining its contribution to the laser frequency noise. This was achieved by multiplying the electrical noise by the current-tuning rate of the laser measured at the corresponding temperature. In Fig. 12.8, the 3-kHz component of the frequency noise assessed from the measured electrical noise is displayed as black crosses. It is found to be well correlated with the frequency noise optically measured using the CO lines. These results tend to show that the laser frequency noise is induced by internal electrical noise in the QCL structure and that the strong increase in frequency noise at low temperatures results from the strong increase in the electrical noise. However, the mechanism that produces the electrical noise in the QCL is not yet well understood. 1/*f* noise is quite typical in semiconductor devices and has been studied for a long time in various experiments,[55] but its origin is generally difficult to identify. Among possible effects, additional current noise in QCLs may originate from the contacts, from lattice scattering,[56] from carriers trapped by material defects,[57] or from fluctuations in electron tunneling through the multiple-barrier QCL structure.[23] Additional experiments, such as the characterization of frequency-noise temperature dependence in other QCLs, possibly with different parameters, will be needed to better understand the origin of frequency noise.

12.8 Conclusion and Outlook

Frequency noise in QCLs has been reviewed based on experimental results obtained recently in our group and in other groups worldwide. QCLs operate on a principle that is different from that of interband diode lasers, resulting in a linewidth enhancement factor α_e that is close to zero. As a consequence, the intrinsic linewidth in QCLs is much narrower than in diode lasers operating at the same output power. Typical intrinsic linewidths in the 300- to 500-Hz range have been assessed for QCLs from the white-noise plateau observed in the high-frequency part of their frequency noise spectrum. These values are in good agreement with the theoretical Schawlow–Townes limit calculated from the physical parameters of these lasers. However, the intrinsic linewidth of QCLs is never observed experimentally because of the large spectral broadening induced by the presence of flicker frequency noise. This flicker noise can have two different contributions, internal or external to the laser.

A first contribution to the QCL frequency noise arises from technical noise that is external to the laser. A critical aspect regarding technical noise is the current source used to drive the QCL. A low-noise current controller is needed to keep the contribution of the technical noise sufficiently low to not

affect the laser frequency noise. In terms of numbers, we showed that a white-current noise of 1 nA/Hz$^{1/2}$ is a typical upper limit tolerable for a laser controller to reach the linewidth inherent to the QCL at the megahertz level. The requirement is even more stringent for the narrowest linewidth free-running QCLs observed to date ($\sim$500-kHz linewidth at about 10 ms, which requires a current noise inferior to 500 pA/Hz$^{1/2}$). These values can slightly vary between different QCLs depending on their current-tuning coefficient, but they represent a good approximation for any QCL. The main mechanism of frequency tuning via the drive current is through thermal effects induced by thermal dissipation in the laser structure. The current noise of the laser controller is thus transformed into frequency noise via the laser dynamic tuning response.

Even in the absence of external frequency noise, the linewidth of QCLs that is experimentally observed is much broader than that given by the Schawlow–Townes formula. Different experimental results tend to show that this frequency noise is induced by internal current noise produced in the laser structure. So far, the origin of the internal current noise in QCLs has not been clearly identified, even if different options have been proposed, such as noise induced in the electrical contacts, noise resulting from lattice scattering, noise from carriers trapped by material defaults, or from fluctuations of electron tunneling through the multiple-barrier QCL structure. Further experimental investigations will likely provide new insights on and, hopefully, soon, clarify this question.

References

1. J. Faist, F. Capasso, D. L. Sivco, C. Sirtori, A. L. Hutchinson, and A. Y. Cho, "Quantum cascade lasers," *Science* **264**, 553–556 (1994).
2. J. Faist, F. Capasso, C. Sirtori, D. L. Sivco, J. N. Baillargeon, A. L. Hutchinson, S. N. Chu, and A. Y. Cho, "High power mid-infrared ($\lambda \sim 5$ μm) quantum cascade lasers operating above room temperature," *Appl. Phys. Lett*. **68**(26), 3680–3682 (1996).
3. J. Faist, C. Gmachl, F. Capasso, C. Sirtori, D. L. Silvco, J. N. Baillargeon, and A. Y. Cho, "Distributed feedback quantum cascade lasers," *Appl. Phys. Lett*. **70**(20), 2670–2672 (1997).
4. M. Beck, D. Hofstetter, T. Aellen, J. Faist, U. Oesterle, M. Illegems, E. Gini, and H. Melchior, "Continuous wave operation of a mid-infrared semiconductor laser at room temperature," *Science* **295**, 301–303 (2002).
5. P. Corrigan, R. Martini, E. A. Whittaker, and C. Bethea, "Quantum cascade lasers and the Kruse model in free space optical communication," *Opt. Express* **17**, 4355–4359 (2009).

6. D. D. Nelson, B. McManus, S. Urbanski, S. Herndon, and M. S. Zahniser, "High-precision measurements of atmospheric nitrous oxide and methane using thermoelectrically cooled mid-infrared quantum cascade lasers and detectors," *Spectrochim. Acta, Part A* **60**, 3325–3335 (2004).
7. D. M. Sonnenfroh, W. T. Rawlins, M. G. Allen, C. Gmachl, F. Capasso, A. L. Hutchinson, D. L. Sivco, J. N. Baillargeon, and A. Y. Cho, "Application of balanced detection to absorption measurements of trace gases with room-temperature, quasi-cw quantum-cascade lasers," *Appl. Opt*. **40**(6), 812–820 (2001).
8. K. Namjou, S. Cai, E. A. Whittaker, J. Faist, C. Gmachl, F. Capasso, D. L. Sivco, and A. Y. Cho, "Sensitive absorption spectroscopy with a room-temperature distributed feedback quantum-cascade laser," *Opt. Lett*. **23**(3), 219–221 (1998).
9. S. Borri, S. Bartalini, P. De Natale, M. Inguscio, C. Gmachl, F. Capasso, D. L. Sivco, and A. Y. Cho, "Frequency modulation spectroscopy by means of quantum-cascade lasers," *Appl. Phys. B* **85**(2–3), 223–229 (2006).
10. B. A. Paldus, T. G. Spence, R. N. Zare, J. Oomens, F. J. M. Harren, D. H. Parker, C. Gmachl, F. Capasso, D. L. Sivco, J. N. Baillargeon, A. L. Hutchinson, and A. Y. Cho, "Photoacoustic spectroscopy using quantum-cascade lasers," *Opt. Lett*. **24**(3), 178–180 (1999).
11. R. Lewicki, G. Wysocki, A. A. Kosterev, and F. K. Tittel, "QEPAS based detection of broadband absorbing molecules using a widely tunable, cw quantum cascade laser at 8.4 μm," *Opt. Express* **15**(12), 7357–7366 (2007).
12. B. A. Paldus, C. C. Harb, T. G. Spence, R. N. Zare, C. Gmachl, F. Capasso, D. L. Sivco, J. N. Baillargeon, A. L. Hutchinson, and A. Y. Cho, "Cavity ringdown spectroscopy using mid-infrared quantum-cascade lasers," *Opt. Lett*. **25**(9), 666–668 (2000).
13. S. H. K. Lee and J. S. Yu, "Thermal effects in quantum cascade lasers at $\lambda \sim 4.6$ μm under pulsed and continuous wave modes," *Appl. Phys. B* **106**(3), 619–627 (2012).
14. A. A. Kosterev, F. K. Tittel, C. Gmachl, F. Capasso, D. L. Sivco, J. N. Baillargeon, A. L. Hutchinson, and A. Y. Cho, "Trace-gas detection in ambient air with a thermoelectrically cooled, pulsed quantum-cascade distributed feedback laser," *Appl. Opt*. **39**(36), 6866–6872 (2000).
15. D. Hofstetter, M. Beck, J. Faist, M. Nägele, and M. W. Sigrist, "Photoacoustic spectroscopy with quantum cascade distributed-feedback lasers," *Opt. Lett*. **26**(2), 888–889 (2001).
16. M. Germer and M. Wolff, "Quantum cascade laser linewidth investigations for high resolution photoacoustic spectroscopy," *Appl. Opt*. **48**(4), B80–B86 (2009).

17. L. S. Rothman, I. E. Gordon, A. Barbe, et al., "The HITRAN 2008 molecular spectroscopic database," *J. Quant. Spectrosc. Radiat. Transfer* **110**, 533–572 (2009).
18. D. Weidmann, L. Joly, V. Parpillon, D. Courtois, Y. Bonetti, T. Aellen, M. Beck, J. Faist, and D. Hofstetter, "Free-running 9.1-μm distributed-feedback quantum cascade laser linewidth measurement by heterodyning with a $C^{18}O_2$ laser," *Opt. Lett*. **28**, 704–706 (2003).
19. S. Bartalini, S. Borri, P. Cancio, A. Castrillo, I. Galli, G. Giusfredi, D. Mazzotti, L. Gianfrani, and P. De Natale, "Observing the intrinsic linewidth of a quantum-cascade laser: Beyond the Schawlow–Townes limit," *Phys. Rev. Lett*. **104**, 083904 (2010).
20. L. Tombez, J. Di Francesco, S. Schilt, G. Di Domenico, J. Faist, P. Thomann, and D. Hofstetter, "Frequency noise of free-running 4.6-μm DFB quantum cascade lasers near room temperature," *Opt. Lett*. **36**(16), 3109–3111 (2011).
21. S. Bartalini, S. Borri, I. Galli, G. Giusfredi, D. Mazzotti, T. Edamura, N. Akikusa, M. Yamanishi, and P. De Natale, "Measuring frequency noise and intrinsic linewidth of a room-temperature DFB quantum cascade laser," *Opt. Express* **19**(19), 17996–18003 (2011).
22. L. Tombez, S. Schilt, J. Di Francesco, P. Thomann, and D. Hofstetter, "Temperature dependence of the frequency noise in a mid-IR DFB quantum cascade laser from cryogenic to room temperature," *Opt. Express* **20**(7), 6851–6859 (2012).
23. S. Borri, S. Bartalini, P. C. Pastor, I. Galli, G. Giusfredi, D. Mazzotti, M. Yamanishi, and P. De Natale, "Frequency-noise dynamics of mid-infrared quantum cascade lasers," *IEEE J. Quantum Electron*. **47**, 984–988 (2011).
24. L. Tombez, S. Schilt, J. Di Francesco, T. Führer, B. Rein, T. Walther, G. Di Domenico, D. Hofstetter, and P. Thomann, "Linewidth of a quantum cascade laser assessed from its frequency noise spectrum and impact of the current driver," *Appl. Phys. B* **109**(3), 407–414 (2012).
25. S. Bartalini, S. Borri, and P. De Natale, "Doppler-free polarization spectroscopy with a quantum cascade laser at 4.3 μm," *Opt. Express* **17**(9), 7440–7449 (2009).
26. A. Gambetta, D. Gatti, A. Castrillo, G. Galzerano, P. Laporta, L. Gianfrani, and M. Marangoni, "Mid-infrared quantitative spectroscopy by comb-referencing of a quantum-cascade-laser: Application to the CO_2 spectrum at 4.3 μm," *Appl. Phys. Lett*. **99**(25), 251107 (2011).
27. A. Hugi, G. Villardes, S. Blaser, H. C. Liu, and J. Faist, "Mid-infrared frequency comb based on a quantum cascade laser," *Nature* **492**, 229–233 (2012).

28. R. Maulini, M. Beck, J. Faist, and E. Gini, "Broadband tuning of external cavity bound-to-continuum quantum-cascade lasers," *Appl. Phys. Lett.* **84**(10), 1659–1661 (2004).
29. K. Knabe, P. A. Williams, F. R. Giorgetta, C. M. Armacost, S. Crivello, M. B. Radunsky, and N. R. Newbury, "Frequency characterization of a swept- and fixed-wavelength external-cavity quantum cascade laser by use of a frequency comb," *Opt. Express* **20**, 12432–12442 (2012).
30. A. Gambetta, D. Gatti, A. Castrillo, N. Coluccelli, G. Galzerano, P. Laporta, L. Gianfrani, and M. Marangoni, "Comb-assisted spectroscopy of CO_2 absorption profiles in the near- and mid-infrared regions," *Appl. Phys. B* **109**(3), 385–390 (2012).
31. S. Borri, I. Galli, F. Cappelli, A. Bismuto, S. Bartalini, P. Cancio, G. Giusfredi, D. Mazzotti, J. Faist, and P. De Natale, "Direct link of a mid-infrared QCL to a frequency comb by optical injection," *Opt. Lett.* **37**, 1011–1013 (2012).
32. A. A. Mills, D. Gatti, J. Jiang, C. Mohr, W. Mefford, L. Gianfrani, M. Fermann, I. Hartl, and M. Marangoni, "Coherent phase lock of a 9 μm quantum cascade laser to a 2 μm thulium optical frequency comb," *Opt. Lett.* **37**, 4083–4085 (2012).
33. F. Cappelli, I. Galli, S. Borri, G. Giusfredi, P. Cancio, D. Mazzotti, A. Montori, N. Akikusa, M. Yamanishi, S. Bartalini, and P. De Natale, "Subkilohertz linewidth room-temperature mid-infrared quantum cascade laser using a molecular sub-Doppler reference," *Opt. Lett.* **37**, 4811–4813 (2012).
34. T. Okoshi, K. Kikuchi, and A. Nakayama, "Novel method for high resolution measurement of laser output spectrum," *Electr. Lett.* **16**, 630–631 (1980).
35. D. S. Elliott, R. Roy, and S. J. Smith, "Extracavity laser band shape and bandwidth modification," *Phys. Rev. A* **26**, 12–18 (1982).
36. P. B. Gallion and G. Debarge, "Quantum phase noise and field correlation in single frequency semiconductor laser systems," *IEEE J. Quantum Electron.* **QE-20**, 343–350 (1984).
37. G. M. Stéphan, T. T. Tam, S. Blin, P. Besnard, and M. Têtu, "Laser line shape and spectral density of frequency noise," *Phys. Rev. A* **71**, 043809 (2005).
38. L. B. Mercer, "1/*f* frequency noise effects on self-heterodyne linewidth measurements," *J. Lightwave Technol.* **9**, 485–493 (1991).
39. N. Bucalovic, V. Dolgovskiy, C. Schori, P. Thomann, G. Di Domenico, and S. Schilt, "Experimental validation of a simple approximation to determine the linewidth of a laser from its frequency noise spectrum," *Appl. Opt.* **51**(20), 4582–4588 (2012).

40. G. Di Domenico, S. Schilt, and P. Thomann, "Simple approach to the relation between laser frequency noise and laser line shape," *Appl. Opt*. **49**, 4801–4807 (2010).

41. T. L. Myers, R. M. Williams, M. S. Taubman, C. Gmachl, F. Capasso, D. L. Sivco, J. N. Baillargeon, and A. Y. Cho, "Free-running frequency stability of mid-infrared quantum cascade lasers," *Opt. Lett*. **27**(3), 170–172 (2002).

42. M. S. Vitiello, L. Consolino, S. Bartalini, A. Taschin, A. Tredicucci, M. Inguscio, and P. De Natale, "Quantum-limited frequency fluctuations in a terahertz laser," *Nature Photonics* **6**, 525–528 (2012).

43. L. D. Turner, K. P. Weber, C. J. Hawthorn, and R. E. Scholten, "Frequency noise characterization of narrow linewidth lasers," *Opt. Comm*. **201**, 391–397 (2002).

44. S. Schilt, N. Bucalovic, L. Tombez, V. Dolgovskiy, C. Schori, G. Di Domenico, M. Zaffalon, and P. Thomann, "Frequency discriminators for the characterization of narrow-spectrum heterodyne beat signals: application to the measurement of a sub-hertz carrier-envelope-offset beat in an optical frequency comb," *Rev. Scient. Instr*. **82**(12), 123116 (2011).

45. A. L. Schawlow and C. H. Townes, "Infrared and optical masers," *Phys. Rev*. **112**, 1940–1949 (1958).

46. C. H. Henry, "Theory of the linewidth of semiconductor lasers," *IEEE J. Quant. Elect*. **QE-18**(2), 259–264 (1982).

47. C. M. Yamanishi, T. Edamura, K. Fujita, and N. Akikusa, "Theory of the intrinsic linewidth of quantum-cascade lasers: hidden reason for the narrow linewidth and line-broadening by thermal photons," *IEEE J. Quant. Electr*. **44**, 12–29 (2008).

48. J. Osinski and J. Buus, "Linewidth broadening factor in semiconductor lasers: An overview," *IEEE J. Quant. Electr*. **QE-23**(1), 9–29 (1987).

49. T. Aellen, R. Maulini, R. Terazzi, N. Hoyler, M. Giovaninni, S. Blaser, L. Hvozdara, and J. Faist, "Direct measurement of the linewidth enhancement factor by optical heterodyning of an amplitude-modulated quantum cascade laser," *Appl. Phys. Lett*. **89**, 091121 (2006).

50. A. Wittmann, Y. Bonetti, M. Fischer, J. Faist, S. Blaser, and E. Gini, "Distributed-feedback quantum-cascade lasers at 9 μm operating in continuous wave up to 423 K," *IEEE Photon. Tech. Lett*. **21**(12), 814–816 (2009).

51. R. M. Williams, J. F. Kelly, J. S. Hartman, S. W. Sharpe, M. S. Taubman, J. L. Hall, F. Capasso, C. Gmachl, D. L. Sivco, J. N. Baillargeon, and A. Y. Cho, "Kilohertz linewidth from frequency-stabilized mid-infrared quantum cascade lasers," *Opt. Lett*. **24**, 1844–1846 (1999).

52. M. S. Taubman, T. L. Myers, B. D. Cannon, R. M. Williams, F. Capasso, C. Gmachl, D. L. Sivco, and A. Y. Cho, "Frequency stabilization of quantum-cascade lasers by use of optical cavities," *Opt. Lett*. **27**, 2164–2166 (2002).
53. M. S. Taubman, T. L. Myers, B. D. Cannon, and R. M. Williams, "Stabilization, injection and control of quantum cascade lasers, and their application to chemical sensing in the infrared," *Spectrochim. Acta A*. **60** (14), 3457–3468 (2004).
54. F. Bielsa, A. Douillet, T. Valenzuela, J.-P. Karr, and L. Hilico, "Narrow-line phase-locked quantum cascade laser in the 9.2 μm range," *Opt. Lett*. **32**, 1641–1643 (2007).
55. G. Bosman, Ed., *Proc. of the 16th International Conference on Noise in Physical Systems and 1/f Fluctuations*, World Scientific, Hackensack, NJ (2001).
56. X. Y. Chen, F. N. Hooge, and M. R. Leys, "The temperature dependence of 1/*f* noise in InP," *Solid-State Elec*. **41**, 1269–1275 (1997).
57. T. Roy, E. X. Zhang, Y. S. Puzyrev, X. Shen, D. M. Fleetwood, R. D. Schrimpf, G. Koblmueller, R. Chu, C. Poblenz, N. Fichtenbaum, C. S. Suh, U. K. Mishra, J. S. Speck, and S. T. Pantelides, "Temperature-dependence and microscopic origin of low frequency 1/*f* noise in GaN/AlGaN high electron mobility transistors," *Appl. Phys. Lett*. **99**, 203501 (2011).

Stéphane Schilt obtained his Master's degree in physics from the Swiss Federal Institute of Technology in Lausanne (EPFL) and his Ph.D. in technical sciences in 2002 from the same institution for his work in trace gas sensing by laser spectroscopy. After a three-year post-doctorate, where he worked on photoacoustic spectroscopy and stabilized lasers, he joined the company IR Microsystems in Lausanne to develop low-cost gas sensors based on near-infrared lasers. Since 2009, he has been senior scientist at Laboratoire Temps-Fréquence at the University of Neuchâtel, Switzerland. His research interests are focused on optical frequency combs for time and frequency metrology, studies of the mechanisms of frequency noise in QCLs, and frequency stabilization of these lasers. He published more than 30 papers in peer-reviewed journals and has coauthored more than 60 contributions at international conferences. He is Associate Editor of *Journal of Spectroscopy*.

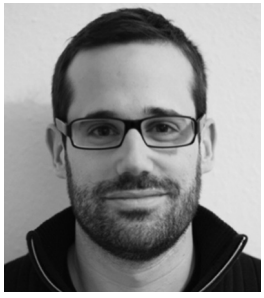

Lionel Tombez received his M.Sc. degree in micro-engineering from EPFL in 2008. From 2008 to 2010 he worked for EM Microelectronic-Marin Ltd, the semi-conductor company of the Swatch Group. In 2010 he joined the Institute of Physics at the University of Neuchâtel as a Ph.D. candidate in the field of low-noise mid-IR semiconductor lasers and optical frequency metrology.

Gianni Di Domenico obtained his Master's degree in physics from the University of Neuchâtel, Switzerland, and his Ph.D. in physics in 2004 from the same institution for his work on continuous beams of laser-cooled atoms applied to time and frequency metrology. After a post-doctorate at the University of Fribourg where he worked on optical magnetometry applied to the measurement of the magnetic field produced by the human heart, he joined the Laboratoire Temps-Fréquence at the University of Neuchâtel, where he works on the Swiss primary frequency standard, a continuous atomic fountain clock developed in collaboration with the Swiss Federal Institute of Metrology. His research interests are cold atomic fountain clocks and optical frequency metrology.

Daniel Hofstetter was an apprentice as an electrical mechanic at Landis & Gyr, Zug, Switzerland, from 1982 to 1986, where he became a physics technician and stayed until 1988. From 1988 to 1993, he studied physics at the Swiss Federal Institute of Technology in Zurich (ETHZ), Switzerland. In his diploma thesis, he carried out photoacoustic spectroscopy on fatty acid vapors. He then moved on and received his Ph.D. from the Paul Scherrer Institute in Zurich, Switzerland in 1996 for work that included the design, fabrication, and testing of a semiconductor-based monolithically integrated double Michelson interferometer for optical displacement measurement. From 1996 to 1998, he was with the XEROX Palo Alto Research Center, Palo Alto, California, USA, developing violet-blue distributed-feedback lasers for scanning and printing applications. In 1998, he joined the group of Prof. Jerome Faist at the Physics Institute of the University of Neuchatel, Switzerland. In 2001, he was awarded the Sofja

Kovalevskaja Prize of the Alexander von Humboldt Foundation, and worked in Ulm, Germany. The following year, he was awarded a position in the Professorship Program of the Swiss National Science Foundation and worked on high-performance mid-infrared quantum cascade lasers and detectors for spectroscopy. Since 2008, he has been a scientific collaborator at the University of Neuchatel. He has published more than 130 papers in international journals and has participated in over 70 conferences.